


Communication

Heterobimetallic 3d-4f (Zn/La) {6,6'-Dimethoxy-2,2'-[naphthalene-2,3-diylbis(nitrilomethylidyne)]diphenolato}-pyridylzinc(II)-tris(nitrato-O,O') lanthanum(III) Monohydrate

Calliope Bee Sue Linden ¹, Nikita Chaudhary ¹, Matthias Zeller ² and Evan R. Trivedi ^{1,*} 

¹ Department of Chemistry, Oakland University, Rochester, MI 48309, USA; jmfarnsworth@oakland.edu (C.B.S.L.); chaudharynikita1@gmail.com (N.C.)

² Department of Chemistry, Purdue University, West Lafayette, IN 47907, USA; zeller4@purdue.edu

* Correspondence: trivedi@oakland.edu; Tel.: +1-248-370-2147

Received: 2 October 2017; Accepted: 15 November 2017; Published: 18 November 2017

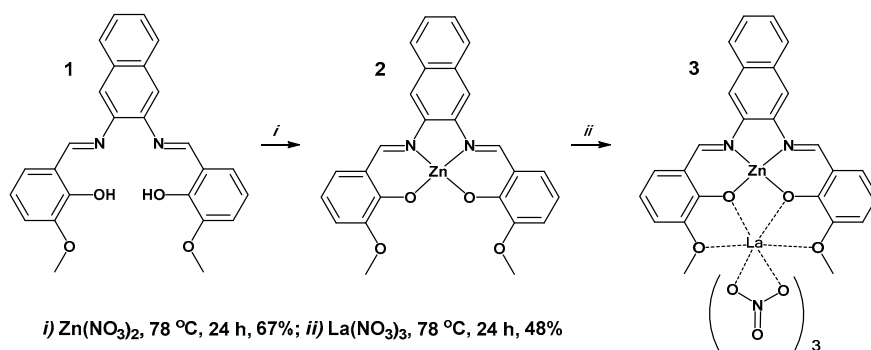
Abstract: Herein, we report the synthesis and structural characterization of a complex with extended aromaticity based on a naphthalene-bridged Schiff base complex with two metal binding pockets. In a first step, the Zn(II) complex (ZnL), {6,6'-dimethoxy-2,2'-[naphthalene-2,3-diylbis(nitrilomethylidyne)]diphenolato}-pyridylzinc(II) was isolated followed by refluxing with lanthanum(III) nitrate to produce the heterobimetallic complex {ZnL[La(NO₃)₃·H₂O]}. Crystals suitable for X-ray diffraction were grown by vapor diffusion of THF into a pyridine solution of the complex. The monoclinic unit cell (P2₁/n) is commensurately modulated along the *c*-axis direction and contains four crystallographically independent molecules with pseudo-translational symmetry being broken by slightly differing orientations of included pyridine and THF solvate molecules. The zinc atom adopts a distorted square pyramidal geometry and sits slightly above the ligand plane, whereas the lanthanum atom adopts an all-face capped trigonal prismatic geometry and sits below the ligand plane. Structural characterization of this diamagnetic complex lays the groundwork for applying these synthetic techniques to the near-infrared emitting lanthanides for practical application.

Keywords: heterobimetallic; rare-earth; schiff base; X-ray crystal structure

1. Introduction

The salen ligand (*N,N'*-bis(salicylidene)ethylenediamine) and associated metal-salen complexes have long been used in homogeneous catalysis [1], with a particular emphasis on their ability to perform enantioselective transformations [2–4]. The attention this ligand system has garnered is due, in part, to its facile synthesis through the condensation of an aldehyde and an amine. More recently, salen type ligands, produced by the condensation of a diamine with *o*-vanillin, have been used to form heterobimetallic complexes. In these systems, a first-row transition metal is bound traditionally in the Schiff base/phenolate (κ^4 -N₂O₂) pocket and a second metal occupies a peripheral (κ^4 -O₂O₂) binding site. These complexes have recently been made with divalent *s*-block metals in the second position [5], but far more examples exist in the literature for heterobimetallic 3d-4f complexes of this type. Choice of lanthanide ion determines applicability; the Gd³⁺ ion produces interesting magnetic materials [6], and Eu³⁺ produces functional luminescent materials [7]. The luminescent ions Yb³⁺ and Nd³⁺ have been well studied with this ligand system for near-infrared luminescence applications [8–13]. Near-infrared luminescence in the region of maximum tissue penetration has potential for fluorescence imaging applications in biology, but most lanthanide complexes of this type require high-energy UV excitation. Extension of the aromatic system of these ligands has the potential to shift this excitation

further towards the visible region, which is more amenable to any future biological applications [14,15]. The naphthalene bridged salen ligand (**1**, Scheme 1) provides this opportunity; metal complexes of this ligand have been previously studied for their anti-cancer properties [16,17], and structural information is available for a related Co^{3+} complex [18]. Described herein is the synthesis and structural characterization of a heterobimetallic $\text{Zn}^{2+}/\text{La}^{3+}$ complex of this naphthalene bridged salen ligand.



Scheme 1. Synthesis of heterobimetallic $\text{Zn}^{2+}/\text{La}^{3+}$ Schiff base complex.

2. Results and Discussion

2.1. Synthetic Details

The naphthalene-bridged Schiff base ligand (**1**) was produced by a modified procedure from the literature in 75% yield (Scheme 1) [17]. The ^1H -NMR (400 MHz, $\text{DMSO}-d_6$) displayed characteristic signals at $\delta = 9.05$ ppm and $\delta = 12.94$, for imino and phenolic protons, respectively. Reaction of the ligand with one equivalent of zinc(II) nitrate resulted in the formation of Zn^{2+} complex (**2**) in 67% isolated yield. Upon addition of zinc(II), the ^1H -NMR resonance for the imino proton shifted to $\delta = 9.15$ ppm and the phenolic resonance disappeared. Further refluxing the Zn^{2+} complex with a slight excess of lanthanum(III) nitrate resulted in a yellow solid that was identified as the heterobimetallic $\text{Zn}^{2+}/\text{La}^{3+}$ complex (**3**).

2.2. X-ray Structure of $\text{Zn}^{2+}/\text{La}^{3+}$ Complex (**3**)

Crystals suitable for X-ray crystallography were grown by vapor diffusion of THF into a pyridine solution of **3** (Figure 1). Each complex contains one $\text{Zn}(\text{II})$ ion in the $\kappa^4\text{-N}_2\text{O}_2$ pocket, sitting 0.52 Å above the plane of the ligand, with an axially bound pyridine molecule, thereby adopting a distorted square pyramidal geometry. The bound $\text{La}(\text{III})$ ion sits on the opposite side of the ligand plane (0.86 Å below) in the $\kappa^4\text{-O}_2\text{O}_2$ pocket; open coordination sites are occupied by one aqua ligand and three nitrates for charge balance. The interatomic distance between the two metals is 3.626 Å [19].

Selected bond distances are found in Table 1, reported here for each crystallographically independent molecule in the unit cell (A–D) and as the average of the four. The Zn – N (imine) bonds are equal and slightly longer than those previously reported using an analogous phenylene bridged ligand (2.05/2.06 vs. 2.03 Å) [13], presumably due to the increased electron donation from the naphthalene bridge reported here. The Zn – O (phenolate) bonds are shorter; the relative bond distances for this binding pocket are consistent with literature values.

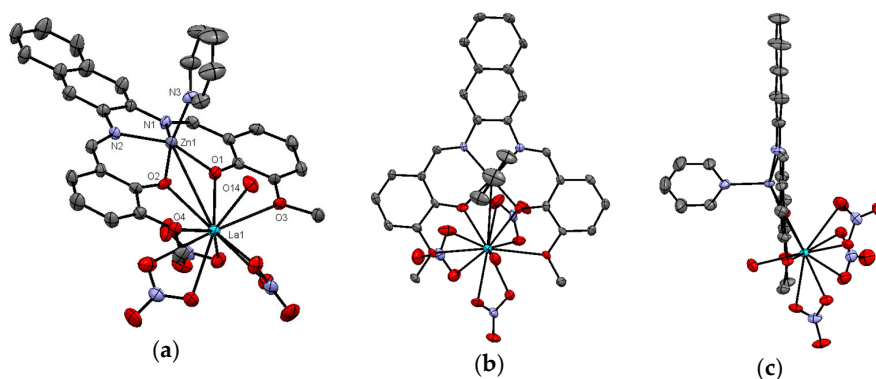


Figure 1. ORTEP diagrams of $\text{Zn}^{2+}/\text{La}^{3+}$ complex (**3**) showing (a) perspective view; (b) top view, along c -axis; and (c) side view, along b -axis. 50% probability ellipsoids, H-atoms omitted. Shown is one of four nearly identical crystallographically independent molecules.

Table 1. Selected metal-ligand bond distances in Å.

Bond	A	B	C	D	Average ¹
Zn–N1	2.067 (6)	2.061 (6)	2.052 (6)	2.058 (6)	2.060
Zn–N2	2.039 (7)	2.049 (6)	2.050 (6)	2.048 (6)	2.050
Zn–N3 (pyridyl)	2.052 (8)	2.050 (19)	2.056 (8)	2.047 (7)	2.044
Zn–O1	1.998(5)	1.998 (5)	1.992 (5)	2.005 (5)	1.998
Zn–O2	2.008 (5)	2.004 (5)	1.993 (5)	1.984 (5)	1.997
La–O1	2.484 (5)	2.466 (5)	2.508 (5)	2.513 (5)	2.493
La–O2	2.507 (5)	2.518 (5)	2.487 (5)	2.488 (5)	2.500
La–O3	2.885 (6)	2.996 (6)	2.895 (6)	3.04 (1)	2.953
La–O4	2.866 (6)	2.875 (5)	2.794 (5)	2.856 (6)	2.848
La–O14 (aqua)	2.504 (7)	2.525 (6)	2.504 (7)	2.499 (6)	2.508

¹ Average bond distance across four independent molecules in unit cell.

The unit cell was found to be monoclinic in the $P2_1/n$ space group, and contains four molecules lined up along the c -axis (Figure 2). The molecules are close to being perfectly translated and related by a pseudo two-fold screw axis incompatible with unit cell shape. Exact translation and rotational symmetry is broken by modulations or disorder of solvate pyridine and THF molecules that are H-bonded to the aqua ligand (See Supporting Information). Layers of metal complex are formed along the a - and b -axes with pyridyl zinc moieties pointing toward the void space between layers; the remaining void space is filled with aforementioned solvent molecules.

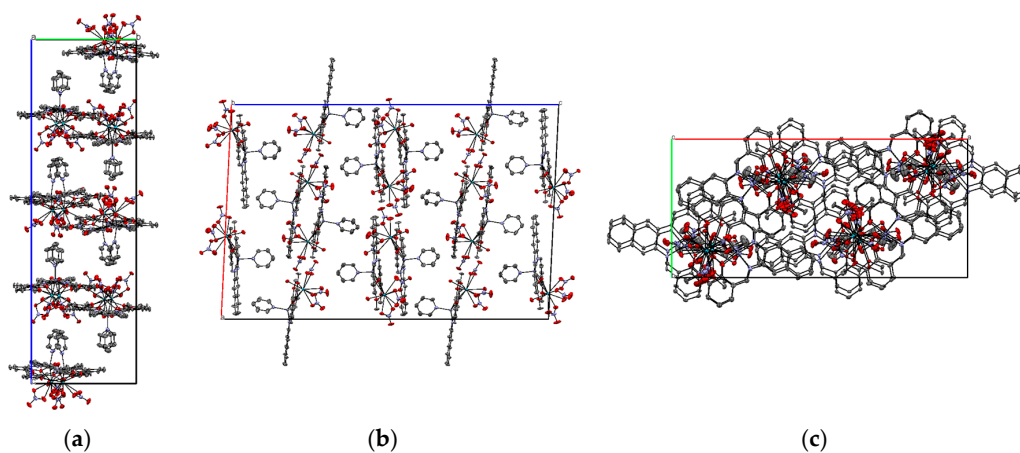


Figure 2. Crystal packing of (**3**) shown along (a) the a -axis; (b) the b -axis; and (c) the c -axis. 50% probability ellipsoids, H-atoms and solvate molecules omitted.

3. Materials and Methods

3.1. General Considerations

Unless otherwise noted, all chemicals and reagents were purchased from Sigma Aldrich (St. Louis, MO, USA). ^1H - and ^{13}C -NMR spectra were recorded on an Avance 400 MHz spectrometer (Bruker, Billerica, MA, USA) and high-resolution ESI mass spectrometry was performed on a 6545 Q-TOF LCMS (Agilent, Santa Clara, CA, USA).

3.2. Synthetic Details

6,6'-Dimethoxy-2,2'-[naphthalene-2,3-diylbis(nitrilomethylidyne)]diphenol (1, L)—To a solution of 2,3-diaminonaphthalene (0.50 g, 3.2 mmol) in absolute ethanol (17 mL), was added *o*-vanillin (1.0 g, 6.6 mmol). The resulting solution was refluxed at 78 °C for 24 h. The reaction mixture was allowed to cool, at which time a bright orange precipitate formed. The product was collected by vacuum filtration and washed with cold ethanol (150 mL) and hexanes (150 mL) and used without further purification (1.0 g, 75%). ^1H -NMR (400 MHz, $\text{DMSO}-d_6$) δ (ppm): 3.82 (s, 6H), 6.94 (m, 2H), 7.15 (dd, $J_{ortho} = 8$ Hz, $J_{meta} = 1$ Hz, 2H), 7.31 (dd, $J_{ortho} = 8$ Hz, $J_{meta} = 1$ Hz, 2H), 7.53 (dd, $J_{ortho} = 6$ Hz, $J_{meta} = 3$ Hz, 2H), 7.92 (s, 2H), 7.97 (dd, $J_{ortho} = 6$ Hz, $J_{meta} = 3$ Hz, 2H), 9.05 (s, 2H), 12.94 (br s, 2H). ^{13}C -NMR (125 MHz, CDCl_3) δ (ppm): 56.4, 115.5, 117.6, 118.7, 119.5, 124.2, 126.5, 127.8, 132.9, 143.0, 148.8, 152.0, 164.4. HR-LCMS (ESI) Calculated for $\text{C}_{26}\text{H}_{23}\text{N}_2\text{O}_4$, $[\text{M} + \text{H}]^+$ 427.1652; found 427.1654. Calculated for $\text{C}_{26}\text{H}_{22}\text{N}_2\text{NaO}_4$ $[\text{M} + \text{Na}]^+$ 449.1472; found 449.1472.

Zn^{2+} complex (2, ZnL)—Ligand (1) (0.23 g, 0.53 mmol) was dissolved in absolute ethanol (20 mL) and zinc(II) nitrate hexahydrate (0.18 g, 0.60 mmol) was added. The resulting solution was refluxed at 78 °C for 24 h, at which time it was allowed to cool. A bright yellow precipitate was collected by vacuum filtration, and washed with cold ethanol (100 mL) and hexanes (25 mL) and used without further purification (0.17 g, 67%). ^1H -NMR (400 MHz, $\text{DMSO}-d_6$) 3.78 (s, 6H), 6.47 (m, 2H), 6.88 (d, $J = 7$ Hz, 2H), 7.07 (d, $J = 7$ Hz, 2H), 7.51 (dd, $J_{ortho} = 6$ Hz, $J_{meta} = 3$ Hz, 2H), 7.94 (dd, $J_{ortho} = 6$ Hz, $J_{meta} = 3$ Hz, 2H), 8.33 (s, 2H), 9.15 (s, 2H).

$\text{Zn}^{2+}/\text{La}^{3+}$ complex (3, ZnL(La))—To a solution of (2) (0.06 g, 0.13 mmol) in absolute ethanol (5 mL) was added lanthanum(III) nitrate hexahydrate (0.09 g, 0.12 mmol). The resulting solution was refluxed at 78 °C for 24 h, after which time a bright yellow precipitate formed. The solid was collected by vacuum filtration, washed with cold ethanol (100 mL), and redissolved in pyridine for crystallization by vapor diffusion of THF. Over the course of two weeks, yellow block crystals were grown and collected by vacuum filtration (0.07 g, 48%).

3.3. X-ray Diffraction Studies

Single crystals of **3** were coated with a trace of mineral oil and quickly transferred to the goniometer head of a Bruker Quest diffractometer (Billerica, MA, USA) with a fixed chi angle, a sealed tube fine focus X-ray tube, single crystal curved graphite incident beam monochromator, a Photon100 CMOS area detector and an Oxford Cryosystems low temperature device (Oxford, UK). Examination and data collection were performed with Mo $\text{K}\alpha$ radiation ($\lambda = 0.71073$ Å) at 150 K. Data were collected, reflections were indexed and processed, and the files scaled and corrected for absorption using APEX3 [20]. Crystals of **3** were found to be four-fold commensurately modulated along the *c*-axis direction, and to be slightly non-merohedrally twinned. The orientation matrices for the two components were identified using the program Cell_Now, with the two components being related by a 180-degree rotation around the real *a*-axis. Integration using SAINT proved problematic due to the excessive multiple overlapping of reflections, resulting in large numbers of rejected reflections. Attempts were made to adjust integration parameters to avoid excessive rejections (through adjustments to integration queue size, blending of profiles, integration box slicing and twin overlap parameters), which led to fewer, but still substantial numbers of, rejected reflections. With no complete data set obtainable through simultaneous integration of both twin domains, the data were

instead integrated in SAINT as if not twinned, with only the major domain integrated, and converted into an hklf 5 type format hkl file after integration using the “Make HKLF5 File” routine as implemented in WinGX. The twin law matrix was used as obtained from SAINT, see above. The Overlap R1 and R2 values used were 0.45, i.e., reflections with a discriminator function less or equal to an overlap radius of 0.45 were counted as overlapped, all others as single. The discriminator function used was the “delta function on index non-integrality”. No reflections were omitted. The transformation matrix used was 1.000 0.000 0.000, 0.000 −1.000 0.000, −0.150 0.000 −1.000.

The space group was assigned and the structure was solved by direct methods using XPREP within the SHELXTL suite of programs [21,22] with the hklf 4 type file, and refined by full-matrix least-squares against F^2 with all reflections using Shelxl2016 [23,24] with the graphical interface Shelxle [25], and using the hklf 5 type file, which resulted in a BASF value of 0.0336(4). No R_{int} value or number of independent reflections were obtainable for the hklf 5 type file using the WinGX routine [26]. The values from the HKLF 4 type refinement are given instead.

The structure is characterized by a commensurate modulation along the c -axis. Four molecules are lined up along this axis, with molecules A and C, and B and D being close to perfectly translated, and molecules A and B, and C and D being related by a pseudo two-fold screw axis incompatible with the unit cell shape. Exact translation and rotational symmetry is broken by modulations and/or disorder of solvate pyridine and THF molecules, and slight modulations of the coordinated nitrate anions. For entity B, both the coordinated, as well as the non-coordinated pyridine molecules were refined as disordered by a rotation around the molecule axis through nitrogen.

For entities A, B and C, the THF molecules H bonded to the metal-coordinated water molecules, while the interstitial THF molecules were refined as disordered over two orientations. For entity B, the two THF molecules were also disordered, with a water molecule H bonded to the more prevalent of the two THF moieties.

All disordered entities were restrained to have a geometry similar to that of at least one other not-disordered entity of the same kind (SAME commands in Shexl). U^{ij} components of ADPs of disordered atoms were restrained to be similar for atoms closer to each other than 1.7 Å. THF O atoms O15a and O15e were constrained to have identical positions and thermal parameters. H atoms attached to carbon atoms were positioned geometrically, and constrained to ride on their parent atoms, with carbon hydrogen bond distances of 0.95 Å for aromatic C-H, 0.99 and 0.98 Å for aliphatic CH_2 and CH_3 moieties, respectively. Methyl H atoms were allowed to rotate, but not to tip to best fit the experimental electron density. Water H atoms were restrained to have O-H distances of 0.84(2) Å. For the partially occupied water molecule H atom positions were restrained based on H-bonding considerations. $U_{\text{iso}}(\text{H})$ values were set to a multiple of $U_{\text{eq}}(\text{C/O})$ with 1.5 for OH and CH_3 , and 1.2 for C-H and CH_2 units, respectively. Subject to these conditions, the occupancy rates refined to values between 0.719(14) and 0.281(14). See atom tables in the cif for all values.

Crystal data for $\text{C}_{31}\text{H}_{27}\text{LaN}_6\text{O}_{14}\text{Zn}\cdot\text{C}_5\text{H}_5\text{N}\cdot 2(\text{C}_4\text{H}_8\text{O})\cdot 0.166(\text{H}_2\text{O})$ ($M = 910.0$ g/mol): monoclinic, space group $P2_1/n$ (no. 14), $a = 29.9571(19)$, $b = 13.9500(9)$, $c = 45.702(3)$, $\alpha = 90^\circ$, $\beta = 92.726(2)^\circ$, $\gamma = 90^\circ$, $V = 19077(2)$ Å³, $Z = 16$, $T = 150$ K, $\mu(\text{MoK}\alpha) = 1.46$ mm^{−1}; $D_{\text{calc}} = 1.585$ g/cm³, 338268 reflections measured ($2.945^\circ \leq \theta \leq 28.283^\circ$), 73,124 unique ($R_{\text{int}} = 0.0611$, $R_{\text{sigma}} = 0.0424$), which were used in all calculations. The final $R1$ was 0.0826 ($I > 2\sigma(I)$) and $wR2$ was 0.2050 (all data).

Complete crystallographic data, in CIF format, have been deposited with the Cambridge Crystallographic Data Centre. CCDC 1577726 contains the supplementary crystallographic data for this paper. These data can be obtained free of charge from The Cambridge Crystallographic Data Centre via www.ccdc.cam.ac.uk/data_request/cif.

Supplementary Materials: The following are available online www.mdpi.com/1422-8599/2017/4/M965, Figure S1: ¹H-NMR spectrum of ligand **1** in DMSO- d_6 , Figure S2: ¹³C-NMR spectrum of ligand **1** in CDCl₃, Figure S3: ¹H-NMR spectrum of ZnL complex **2**, Figure S4: Crystal packing with solvent molecules included, Figure S5: Perspective view showing H-bonded solvent molecules (THF and pyridine).

Acknowledgments: The authors would like to acknowledge generous funding from the Michigan Space Grant Consortium (Research Seed Grant, Evan R. Trivedi), the Oakland University Research Committee (Undergraduate Student Research Award, Jake M. Farnsworth) and the Oakland University Office of the Provost & Vice President for Academic Affairs (Provost Undergraduate Research Award, Jake M. Farnsworth). This material is based in part upon work supported by the National Science Foundation through the Major Research Instrumentation Program under Grant No. CHE 1625543. (Funding for the single crystal X-ray diffractometer).

Author Contributions: E.R.T. conceived and designed the experiments; C.B.S.L., N.C., and M.Z. performed the experiments; M.Z. and E.R.T. analyzed the data; C.B.S.L., M.Z., and E.R.T. wrote the paper.

Conflicts of Interest: The authors declare no conflict of interest.

References and Note

1. Cozzi, P.G. Metal-salen schiff base complexes in catalysis: Practical aspects. *Chem. Soc. Rev.* **2004**, *33*, 410–421. [[CrossRef](#)] [[PubMed](#)]
2. Sigman, M.S.; Jacobsen, E.N. Enantioselective Addition of Hydrogen Cyanide to imines Catalyzed by a Chiral (Salen)Al(III) Complex. *J. Am. Chem. Soc.* **1998**, *120*, 5315–5316. [[CrossRef](#)]
3. White, D.E.; Tadross, P.M.; Lu, Z.; Jacobsen, E.N. A broadly applicable and practical oligomeric (salen)Co catalyst for enantioselective epoxide ring-opening reactions. *Tetrahedron* **2014**, *70*, 4165–4180. [[CrossRef](#)] [[PubMed](#)]
4. Larrow, J.F.; Jacobsen, E.N. Asymmetric processes catalyzed by chiral (salen)metal complexes. *Top. Organomet. Chem.* **2004**, *6*, 123–152. [[CrossRef](#)]
5. Hari, N.; Jana, A.; Mohanta, S. Syntheses, crystal structures and esi-ms of mononuclear-Dinuclear, trinuclear and dinuclear based one-dimensional copper(II)-s block metal ion complexes derived from a 3-ethoxysalicylaldehyde-diamine ligand. *Inorg. Chim. Acta* **2017**, *467*, 11–20. [[CrossRef](#)]
6. Deng, X.-W.; Cai, L.-Z.; Zhu, Z.-X.; Gao, F.; Zhou, Y.-L.; Yao, M.-X. Synthesis, structures and magnetic properties of chiral 3d-3d'-4f heterotrimetallic complexes based on [(Tp*)Fe(CN)₃][−]. *New J. Chem.* **2017**, *41*, 5988–5994. [[CrossRef](#)]
7. Liu, L.; Li, H.; Su, P.; Zhang, Z.; Fu, G.; Li, B.; Lu, X. Red to white polymer light-emitting diode (PLED) based on Eu³⁺-Zn²⁺-Gd³⁺-containing metallopolymer. *J. Mater. Chem. C* **2017**, *5*, 4780–4787. [[CrossRef](#)]
8. Pushkarev, A.P.; Balashova, T.V.; Kukinov, A.A.; Arsenyev, M.V.; Yablonskiy, A.N.; Kryzhkov, D.I.; Andreev, B.A.; Rumyantsev, R.V.; Fukin, G.K.; Bochkarev, M.N. Sensitization of NIR luminescence of Yb³⁺ by Zn²⁺ chromophores in heterometallic complexes with a bridging schiff-base ligand. *Dalton Trans.* **2017**, *46*, 10408–10417. [[CrossRef](#)] [[PubMed](#)]
9. Su, P.; Fu, G.; Liu, L.; Feng, W.; Lü, X. Single-nodal linking for Zn²⁺-Nd³⁺-containing metallopolymer with efficient near-infrared (NIR) luminescence. *Inorg. Chem. Commun.* **2017**, *83*, 36–39. [[CrossRef](#)]
10. Lu, X.Q.; Feng, W.X.; Hui, Y.N.; Wei, T.; Song, J.R.; Zhao, S.S.; Wong, W.Y.; Wong, W.K.; Jones, R.A. Near-infrared luminescent, neutral, cyclic Zn₂Ln₂ (Ln = Nd, Yb, and Er) complexes from asymmetric salen-type schiff base ligands. *Eur. J. Inorg. Chem.* **2010**, 2714–2722. [[CrossRef](#)]
11. Yang, X.P.; Jones, R.A.; Wu, Q.Y.; Oye, M.M.; Lo, W.K.; Wong, W.K.; Holmes, A.L. Synthesis, crystal structures and antenna-like sensitization of visible and near infrared emission in heterobimetallic Zn-Eu and Zn-Nd schiff base compounds. *Polyhedron* **2006**, *25*, 271–278. [[CrossRef](#)]
12. Wong, W.-K.; Yang, X.; Jones, R.A.; Rivers, J.H.; Lynch, V.; Lo, W.-K.; Xiao, D.; Oye, M.M.; Holmes, A.L. Multinuclear luminescent schiff-base zn-nd sandwich complexes. *Inorg. Chem.* **2006**, *45*, 4340–4345. [[CrossRef](#)] [[PubMed](#)]
13. Lo, W.K.; Wong, W.K.; Wong, W.Y.; Guo, J.P.; Yeung, K.T.; Cheng, Y.K.; Yang, X.P.; Jones, R.A. Heterobimetallic Zn(II)-Ln(III) phenylene-bridged schiff base complexes, computational studies, and evidence for singlet energy transfer as the main pathway in the sensitization of near-infrared Nd³⁺ luminescence. *Inorg. Chem.* **2006**, *45*, 9315–9325. [[CrossRef](#)] [[PubMed](#)]
14. Eliseeva, S.V.; Buenzli, J.-C.G. Lanthanide luminescence for functional materials and bio-sciences. *Chem. Soc. Rev.* **2010**, *39*, 189–227. [[CrossRef](#)] [[PubMed](#)]
15. Bunzli, J.C.G.; Eliseeva, S.V. Lanthanide NIR luminescence for telecommunications, bioanalyses and solar energy conversion. *J. Rare Earths* **2010**, *28*, 824–842. [[CrossRef](#)]

16. Ansari, K.I.; Grant, J.D.; Woldemariam, G.A.; Kasiri, S.; Mandal, S.S. Iron(III)-salen complexes with less DNA cleavage activity exhibit more efficient apoptosis in MCF7 cells. *Org. Biomol. Chem.* **2009**, *7*, 926–932. [[CrossRef](#)] [[PubMed](#)]
17. Ansari, K.I.; Grant, J.D.; Kasiri, S.; Woldemariam, G.; Shrestha, B.; Mandal, S.S. Manganese(III)-salens induce tumor selective apoptosis in human cells. *J. Inorg. Biochem.* **2009**, *103*, 818–826. [[CrossRef](#)] [[PubMed](#)]
18. Yu, Z.; Kuroda-Sowa, T.; Nabei, A.; Maekawa, M.; Okubo, T. {6,6'-dimethoxy-2,2'-[naphthalene-2,3-diylbis(nitrilomethylidyne)]diphenolato}thiocyanatocobalt(III) diethyl ether dichloromethane solvate. *Acta Crystallogr. Sect. E Struct. Rep. Online* **2009**, *65*, m257–m258. [[CrossRef](#)] [[PubMed](#)]
19. Average interatomic distance across four independent molecules in unit cell.
20. Bruker. *Apex3 v2016.9-0*, SAINT V8.37A; Bruker AXS Inc.: Madison, WI, USA, 2013/2014.
21. *SHELXTL Suite of Programs*, version 6.14; Bruker Advanced X-ray Solutions; Bruker AXS Inc.: Madison, WI, USA, 2000–2003.
22. Sheldrick, G.M. A short history of shelx. *Acta Crystallogr. Sect. A* **2008**, *64*, 112–122. [[CrossRef](#)] [[PubMed](#)]
23. Sheldrick, G.M. University of Göttingen: Göttingen, Saxony, Germany. Personal communication, 2016.
24. Sheldrick, G.M. Crystal structure refinement with SHELXL. *Acta Crystallogr. Sect. C Struct. Chem.* **2015**, *71*, 3–8. [[CrossRef](#)] [[PubMed](#)]
25. Hubschle, C.B.; Sheldrick, G.M.; Dittrich, B. ShelXle: A Qt graphical user interface for SHELXL. *J. Appl. Crystallogr.* **2011**, *44*, 1281–1284. [[CrossRef](#)] [[PubMed](#)]
26. Farrugia, L.J. Wingx and ortep for windows: An update. *J. Appl. Crystallogr.* **2012**, *45*, 849–854. [[CrossRef](#)]



© 2017 by the authors. Licensee MDPI, Basel, Switzerland. This article is an open access article distributed under the terms and conditions of the Creative Commons Attribution (CC BY) license (<http://creativecommons.org/licenses/by/4.0/>).